

Communication

# Eight-Wavelength-Switchable Narrow Linewidth Erbium-Doped Fiber Laser Based on Cascaded Superimposed High-Birefringence Fiber Bragg Grating

Dongyuan Li <sup>1</sup>, Ting Feng <sup>1,\*</sup> , Weiwei Sun <sup>1</sup>, Shengbao Wu <sup>1</sup>, Fengping Yan <sup>2</sup>, Qi Li <sup>3</sup> and Xiaotian Steve Yao <sup>1</sup>

<sup>1</sup> Photonics Information Innovation Center, Hebei Provincial Center for Optical Sensing Innovations, College of Physics Science and Technology, Hebei University, Baoding 071002, China

<sup>2</sup> School of Electronic and Information Engineering, Beijing Jiaotong University, Beijing 100044, China

<sup>3</sup> Sichuan Strongest Laser Technology Co., Ltd., Chengdu 610000, China

\* Correspondence: wlxyft@hbu.edu.cn

**Abstract:** A narrow-linewidth eight-wavelength-switchable erbium-doped fiber laser is proposed, and its performance is demonstrated. A cascaded superimposed high-birefringence fiber Bragg grating is used to determine the lasing wavelengths. The combination of a Fabry–Pérot filter and a single-coupler ring is adopted to achieve the single-longitudinal-mode (SLM) oscillation. By introducing the enhanced polarization-hole-burning effect to suppress the gain competition between different wavelength lasers, the stable lasing output is guaranteed. When the pump power is 200 mW, by adjusting the polarization controller to balance the gain and loss in the laser cavity, 24 switchable lasing modes are achieved, including 8 single-wavelength operations and 16 dual-wavelength operations with orthogonal polarization states. For single-wavelength operations, every laser is in the SLM lasing state, with a high stabilized optical spectrum, a linewidth of approximately 1 kHz, an optical signal-to-noise ratio (OSNR) as high as 73 dB, a relative intensity noise of less than  $-150$  dB/Hz, and very good polarization characteristics. For dual-wavelength operations, the lasers also have a stable spectrum and an OSNR as high as 65 dB. The proposed fiber laser has a wide range of applications, including long-haul coherence optical communication, optical fiber sensing, and dense wavelength-division-multiplexing.

**Keywords:** fiber laser; wavelength-switching; single-longitudinal-mode; narrow linewidth



**Citation:** Li, D.; Feng, T.; Sun, W.; Wu, S.; Yan, F.; Li, Q.; Yao, X.S.

Eight-Wavelength-Switchable Narrow Linewidth Erbium-Doped Fiber Laser Based on Cascaded Superimposed High-Birefringence Fiber Bragg Grating. *Electronics* **2022**, *11*, 3688. <https://doi.org/10.3390/electronics11223688>

Academic Editor: Ju Han Lee

Received: 25 October 2022

Accepted: 9 November 2022

Published: 10 November 2022

**Publisher's Note:** MDPI stays neutral with regard to jurisdictional claims in published maps and institutional affiliations.



**Copyright:** © 2022 by the authors. Licensee MDPI, Basel, Switzerland. This article is an open access article distributed under the terms and conditions of the Creative Commons Attribution (CC BY) license (<https://creativecommons.org/licenses/by/4.0/>).

## 1. Introduction

The single-longitudinal-mode (SLM) fiber laser has been widely studied. Due to its high light conversion efficiency, low noise, high coherence, and all optical fiber structure, the SLM narrow-linewidth fiber laser has a great application value in coherent optical communication, optical fiber sensing, microwave photonics, and LiDAR [1–5]. In recent years, SLM narrow-linewidth fiber lasers, capable of wavelength-tuning and multi-wavelength-switching, were studied [6–11]. These lasers will be further applied in several domains, such as dense wavelength-division-multiplexing optical communication, multi-parameter optical fiber sensing, etc.

Several methods allowing to obtain multi-wavelength fiber laser output have been reported. For example, a multi-channel optical filter has been introduced into a main-ring cavity (MRC), including a waveguide micro-ring [12], Sagnac ring mirror [13], micro-ring-resonator [6], Mach-Zehnder interferometer (MZI) [14], core-offset few-mode fiber filter [15], and fiber Bragg grating (FBG) with multi-channels [10,11,16,17]. Since the multi-channel FBG has many advantages, such as simple preparation, high stability, and narrow-band filtering, it is widely applied in fiber lasers to perform multi-wavelength lasing. The strong gain competition is introduced into the laser cavity among different lasing wavelengths, due to the homogenous broadening effect of the rare-earth-doped gain fibers. In order to

achieve the simultaneous output of lasers with different wavelengths, the gain and loss of each laser should be balanced using an effective stabilizing mechanism. The stable multi-wavelength lasing output was achieved due to the introduction of the following mechanisms in a fiber laser cavity: a light amplitude equalizer [18,19], four-wave mixing effect [20], and polarization-hole-burning (PHB) effect [10,11,21]. The high-birefringence FBG (HBFBG), which has two reflecting filtering channels with orthogonal polarization states, combines the PHB effect in the gain fiber to mitigate gain competition between two lasing wavelengths. In addition, by adjusting the light polarization in the MRC, the polarization-dependent-loss (PDL) can be introduced at the HBFBG. Then the stable switchable lasing outputs with two different wavelengths and orthogonal polarization states and the dual-wavelength lasing output can be obtained. By reasonably designing the HBFBG structure, our group [11] used a superimposed HBFBG (SI-HBFBG) to select the lasing wavelengths in an erbium-doped fiber laser (EDFL), and achieved a stable switchable operation among four lasing wavelengths and fifteen lasing states [11]. Based on the good polarization characteristics of HBFBG, it is expected to design polarization-dependent filters with more channels to develop multi-wavelength-switchable fiber lasers.

The SLM fiber laser can be developed by two short linear cavity structures, including the distributed feedback (DFB) and the distributed Bragg reflector (DBR) [22,23], as well as a ring cavity structure with an ultra-narrow-band filter [10,11,24], such as a compound-ring cavity [10,11,25,26], an FBG [27,28], and an unpumped rare-earth-doped fiber-based saturable absorber (SA) [9,24]. Having a simple structure and a stable operation, DFB and DBR are still the main types of fiber lasers on the market [4]. However, using these lasers, it is difficult to satisfy some needs in many specific applications, and the ultra-narrow-linewidth laser output requires a complex frequency stabilization. However, the length of the ring cavity is not strict. Therefore, the higher power and ultra-narrow-linewidth laser output can be achieved, and various functional devices can be inserted into the ring cavity to achieve a multi-function lasing operation. Unfortunately, the longtime stability of the above ultra-narrow-band SLM filters is the main current problem, which limits their real applications. The Fabry–Pérot (F-P) filter is a high finesse comb filter, often used for wavelength calibration and frequency stabilization [4,29]. It has a large operating bandwidth and a stable performance, and it has developed into a mature commercial filter. By reasonably designing the free spectrum range (FSR) and full-width at half-maximum (FWHM) of the F-P filter, besides the use of a multi-channel filter to select the lasing wavelengths, it is expected to develop a multi-wavelength-switchable SLM narrow-linewidth fiber laser having a high performance and a stable operation [30].

In this paper, an eight-wavelength-switchable EDFL (8WS-EDFL) with a high performance is proposed and demonstrated. A new filter of cascaded SI-HBFBG (CSI-HBFBG) as a polarization-dependent eight-channel wavelength selector is introduced in the MRC. A length of gain erbium-doped fiber (EDF), coiled in a three-loop polarization controller (TL-PC), can produce bending-induced birefringence, and then enhance the PHB effect. The switching operation among the different single-wavelength lasing outputs and different multi-wavelength lasing outputs can be achieved by adjusting the polarization states of the lasers in the cavity. The combination of an F-P filter with custom-made FSR and FWHM and a single-coupler ring (SCR) made by an optical coupler (OC), is adopted to select the SLM. When the pump power is 200 mW, by adjusting two TL-PCs, the 8WS-EDFL can be switched among 24 lasing states, including 8 single-wavelength operations and 16 dual-wavelength operations. In this paper, the characteristics of the eight single-wavelength operations are studied in detail, including the stability of the optical spectrum, SLM, linewidth, relative intensity noise (RIN), and polarization.

## 2. Experimental Setup and Principle

The configuration of the proposed 8WS-EDFL is shown in Figure 1. It includes a 980 nm laser diode (LD, Connect VLSS-980, Shanghai, China), a wavelength division multiplexer (WDM, 980/1550 nm), a CSI-HBFBG, a 2.9 m-long EDF, a 90:10 OC1, an SCR, and an F-P

filter. The EDF (Fibercore M12-980-125, MI, USA) is pumped by the LD and coiled into the three plates of the TL-PC1 to achieve  $1/4$ ,  $1/2$ , and  $1/4$  wave plates, respectively. In addition, the fiber loops in the TL-PC1 introduce internal stress in the EDF to induce a birefringence, which depends on the radii of the EDF and the fiber loops together. Note that the standard diameter of the three plates of the TL-PC is 56 mm. A bigger plate diameter for the fiber coiling will induce inadequate birefringence in the EDF, and a smaller diameter of fiber coiling can introduce larger bending loss to the EDF. According to the study presented in [21], although the incident lights of the different lasing wavelengths have the same linear polarization state in the EDF, they will have different polarization directions based on the effective phase difference between the fast and slow axes, which can introduce an enhanced PHB effect in the EDF. The lasers having different polarization directions can use different subsets of erbium ions due to the PHB effect. Therefore, the competition among the different lasers can be significantly mitigated to achieve a stable lasing output [10,11]. Moreover, the CSI-HBFBG is highly polarization-dependent, as described in the following section, and its different wavelength channels reflect lights with different linear polarizations, which can enhance the PHB effect of the lasers at different wavelengths in the EDF. The CSI-HBFBG is introduced as an eight-channel reflecting filter by a 3-port optical circulator, which can also enable a unidirectional light oscillation.

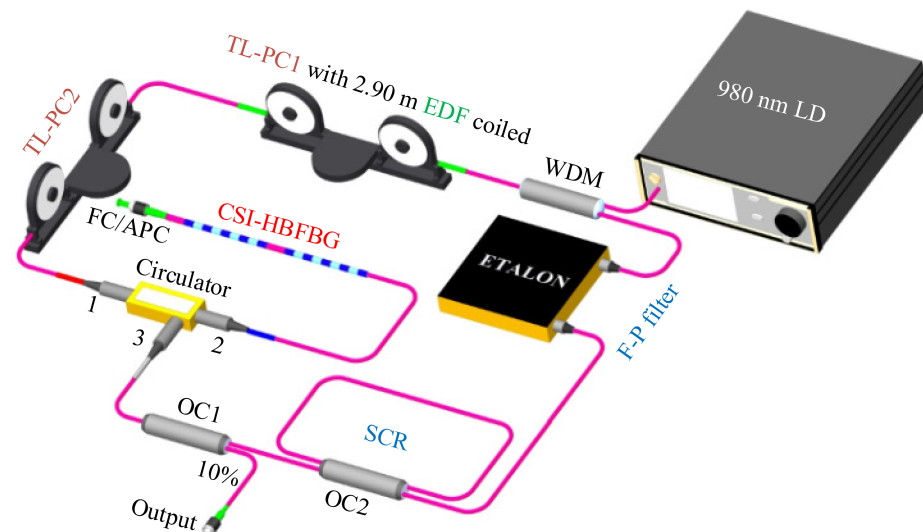


**Figure 1.** Schematic of the proposed 8WS-EDFL. LD: laser diode; WDM: wavelength division multiplexer; EDF: erbium-doped fiber; TL-PC: three-loop polarization controller; CSI-HBFBG: cascaded superimposed high-birefringence fiber Bragg grating; OC: optical coupler; SCR: single coupler ring; F-P filter: Fabry-Pérot filter.

The CSI-HBFBG was fabricated using the phase-mask method. A uniform FBG was first inscribed in a polarization-maintaining fiber (PMF). Then, at the same fiber position, the second FBG was inscribed after a suitable tensile force,  $f_T$ , was applied to the PMF. This is equivalent to inscribing two FBGs, in turn using two uniform phase-masks with different periods. Since the PMF had a high birefringence, this process was equivalent to the fabrication of two HBFBGs at the identical position of the PMF. The above processes can fabricate the first SI-HBFBG, and by appropriately adjusting the tensile force,  $f_T$ , applied to the PMF to change the period of the second inscribed FBG, the SI-HBFBG can have four reflection channels, all with different central wavelengths. Similarly, the other SI-HBFBG was fabricated in the other PMF, by inscribing the third and fourth FBG, in turn with tensile-forces of  $2f_T$  and  $3f_T$  applied to the fiber, respectively. The CSI-HBFBG was made by fusion splicing two SI-HBFBGs together with a  $0^\circ$  polarization-axial-offset. The CSI-HBFBG was used as an eight-channel reflection filter for primary determination of the eight lasing wavelengths in the 8WS-EDFL. It is measured based on the method presented in [10]. The

pure reflection optical spectrum of the CSI-HBFBG is given in Figure 2a. The resolution and data sampling interval of the OSA (OSA, Yokogawa AQ6370D, Tokyo, Japan) used are 0.02 nm and 0.001 nm, respectively. The center wavelengths of the eight reflecting channels are approximately 1553.681 nm, 1554.330 nm, 1555.056 nm, 1555.745 nm, 1556.683 nm, 1557.333 nm, 1557.981 nm, and 1558.629 nm. The reflecting channels 1, 3, 5 and 7 with the same polarization state are located on a polarization-axis of PMF. The channels 2, 4, 6 and 8 are located on the other polarization-axis of PMF, which reflect lights with the polarization state orthogonal to that of the lights reflected by channels 1, 3, 5, and 7. The corresponding reflections of the eight reflecting channels are highly polarization-dependent. The highest reflectivity for every channel is shown in Figure 2a. It has been deduced in [21] that different lasers with the same polarization state have different polarization states and gains after passing the EDF due to the enhanced PHB effect in the EDF. Therefore, the different lasing wavelengths have different PDLs in the CSI-HBFBG for different channels at the same polarization axis of the EDF, and the lasers can be switched among the different lasing wavelengths. Note that, for obtaining a similar output performance for all lasers, the fiber distance between two SI-HBFBGs should be as short as possible to decrease the effective lasing cavity length difference for all eight channels of the CSI-HBFBG.

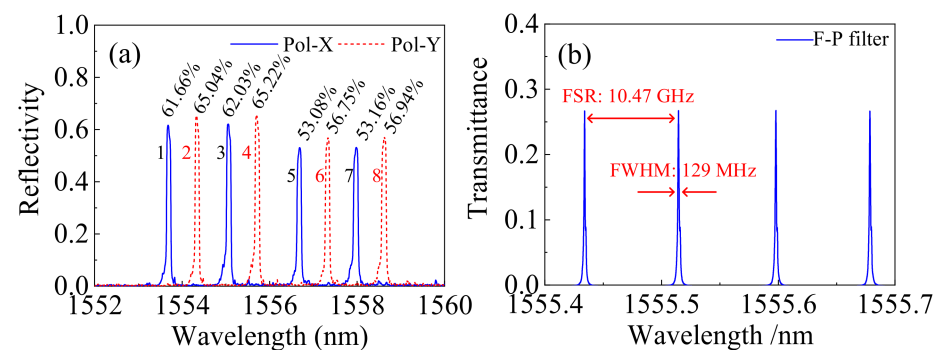


**Figure 2.** (a) Pure reflection spectrum of CSI-HBFBG measured by polarized light in a normalized linear scale. (b) Transmission spectrum of the F-P filter.

The length of the MRC is approximately 14.05 m, corresponding to a longitudinal-mode spacing of almost 14.55 MHz. A system composed of a wavelength-swept laser (Yenista T100s-HP, Lannion, France), a 400 MHz photodetector (PD, Thorlabs PDB470C, NJ, USA), and a data acquisition card (DAQ, Measurement Computing Cor. USB-1602HS, MA, USA) was used to measure the transmission spectrum of the F-P filter. The FSR and FWHM of the F-P filter are, respectively, 10.47 GHz and 129 MHz, as shown in Figure 2b. The FSR of the F-P filter is close to the FWHM ( $\sim 12.5$  GHz) of every channel of the CSI-HBFBG. The FWHM of the F-P filter, which is larger than the longitudinal-mode spacing of the MRC, cannot guarantee a stable SLM operation. The SCR filter, which is made by OC2, is introduced in the MRC to expand the longitudinal-mode spacing of the laser. The coupling ratio and insertion loss of the SCR are 50% and 0.15 dB, respectively. The SCR length is 2 m, corresponding to an FSR of 102.18 MHz (expressed in Equation (1)), which is 0.5–1 times the FWHM of the F-P filter.

$$FSR = c/n_{\text{eff}}L, \quad (1)$$

where  $c$  is the speed of light in vacuum and  $n_{\text{eff}} = 1.468$  is the effective refractive index of the laser propagation in single-mode fibers (SMF).

The FWHM ( $\Delta\nu_{\text{SCR}}$ ) of the SCR is calculated as in [31]:

$$\Delta\nu_{\text{SCR}} = c\delta/2\pi n_{\text{eff}}L, \quad (2)$$

where  $\delta = \ln(I_{\text{in}}/I_{\text{out}})$  is the one-way loss of the cavity, and  $I_{\text{in}}$  and  $I_{\text{out}}$  are the launched and output laser intensities, respectively.

The FWHM of the SCR is 11.79 MHz, which is less than the longitudinal-mode spacing of the MRC and can only allow a longitudinal-mode to pass with low loss. Therefore, according to above analysis, the proposed 8WS-EDFL can have a stable SLM operation.

### 3. Experimental Results and Discussion

The proposed 8WS-EDFL system was constructed on an ordinary metal optical table and measured under room temperature. Considering the filtering characteristics of the CSI-HBFBG, F-P filter and SCR are independent of the input power, a pump power of 200 mW was used for the demonstration. By adjusting two TL-PCs, eight wavelength-switchable lasing operations for the 8WS-EDFL were obtained, as shown in Figure 3a. The central wavelengths of the eight lasers ( $\lambda_1$  to  $\lambda_8$ ) were 1553.750 nm, 1554.410 nm, 1555.065 nm, 1555.712 nm, 1556.711 nm, 1557.367 nm, 1558.018 nm, and 1558.693 nm, which are basically consistent with the central wavelengths of the corresponding channels of the CSI-HBFBG. Figure 3b shows the medium-term running stability lasing at  $\lambda_2$  in a measurement time span of approximately 100 min, measured by repeatedly scanning the OSA with a 0.02 nm resolution and 0.001 nm data sampling interval. It can be seen that the wavelength fluctuation ( $f_{\lambda_2}$ ) is less than 0.001 nm, the power fluctuation ( $f_{p_2}$ ) is less than 0.218 dB, the OSNR is higher than 73 dB, and the side-mode suppression ratio (SMSR) is larger than 56 dB. The output characterizations of all eight lasers are presented in Table 1. It can be clearly observed that the power fluctuations of some lasers ( $\lambda_1$  and  $\lambda_5$ ) are significantly higher than other lasers, and the OSNRs of some lasers ( $\lambda_6$  and  $\lambda_8$ ) are significantly lower than other lasers. On the one hand, this is because it cannot be ensured that the polarization states of all the lasing wavelengths have the best adjustment, and for a system lacking professional temperature compensation and vibration isolation packaging the power fluctuation of some lasing wavelength may increase due to the violent vibration of the surrounding. On the other hand, the reflections of the CSI-HBFBG's different channels are different, the overlap integrals between the different channels of the CSI-HBFBG and corresponding channels of the F-P filter are different, and the PDLs induced by the adjustment of the polarization states of different lasers at CSI-HBFBG are different, which all may cause some lasing wavelengths to have a low Q value of oscillation, and thus their OSNRs are lower than other lasers. In addition, when a wavelength lasing is adjusted to the output with the lowest loss, the other wavelength lasings cannot achieve complete polarization extinction. Therefore, as can be seen in Figure 3, the channels without lasing are still to some extent at an intensity beyond the noise background, which induces the SMSR of every laser to be lower than its OSNR. However, the SMSR for every laser can be further increased through increasing the reflectivity of every channel of the CSI-HBFBG to approach 100% as much as possible, and using another type of EDF with a higher pump efficiency. It should be noted that, in theory, if more than two SI-HBFBGs with different reflection channels are cascaded to fabricate the CSI-HBFBG, more lasing wavelengths for the fiber laser can be obtained. However, too many reflection channels located on the same polarization axis of the PMF will make switching between the different lasing wavelengths difficult and will degrade the anti-disturbance ability of the fiber laser. One may need to do a trade-off between the attainable number of lasing wavelengths and the performance of every switchable lasing operation.

The SLM characteristics at all eight lasing wavelengths were investigated by a scanning F-P interferometer with an FSR of 1.5 GHz and a resolution of 7.5 MHz at the same pump power, as shown in Figure 4, where the red sawtooth wave is the driving voltage signal of the interferometer. As can be seen, in a driving signal period of the F-P interferometer, there are only two lasing modes captured for each lasing wavelength, indicating that the 8WS-EDFL can be in SLM operation at every lasing wavelength.

In addition, the characteristics of the SLM operations at eight lasing wavelengths were further investigated using the self-homodyne method. The RF beating spectra at eight lasing wavelengths were measured using a 400 MHz PD and a radio frequency (RF) electrical spectrum analyzer (ESA, Keysight N9010A, Keysight Technologies, Santa Rosa,

CA, USA), as shown in Figure 5a. We can see that, in a ~10 min measurement time and using the maximum-hold (MH) mode of the ESA for measurement, there was no obvious beating signal captured for every lasing wavelength. The capacity of the F-P filter and SCR was then studied. When the F-P filter and SCR were replaced by a length of SMF to maintain the original MRC's length, and then measured every laser output again, numerous beating signals are seen for each lasing, as shown in Figure 5b. That indicates the lasers all operated in a multi-longitudinal-mode state. In addition, the mode-hopping characteristics of the eight lasing wavelengths were measured using a delayed self-heterodyne measurement system (DSHMS), as shown in Figure 6, where the MZI (made of OC3 and OC4) consists of a 200 MHz acoustic optical modulator (AOM), a PC, and a 100 km SMF (delay fiber) in two arms. The light polarization state in the MZI can be adjusted using the PC to obtain the best contrast of interference fringes. Figure 5c,d, respectively, show the beating results in the ranges of 0–250 MHz and 175–225 MHz, using a 1 GHz PD and the MH mode of the ESA with a measurement time of ~30 min. Considering a 100 km fiber was used in the MZI to provide enough time delay, any mode-hopping of the lasing operation could be captured theoretically. However, only a beating signal at 200 MHz was captured (Figure 5c,d), which was introduced by the AOM. Since the longitudinal-mode spacing in the MRC is approximately 14.6 MHz, it can be concluded that the proposed 8WS-EDFL is in stable SLM operation without mode-hopping during a long time at each lasing wavelength.

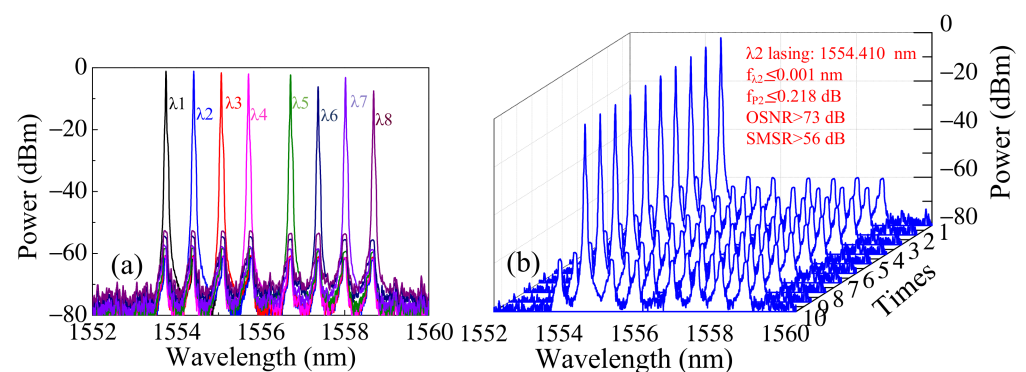


**Figure 3.** (a) 8WS-EDFL laser output spectra of the single-wavelength-switchable operations measured by OSA. (b) Spectral stability of the λ2 lasing.

**Table 1.** Performance parameters of the single-wavelength lasing switchable operations.

Lasing Wavelength	λ1	λ2	λ3	λ4	λ5	λ6	λ7	λ8
Center wavelength/nm	1553.750	1554.410	1555.065	1555.712	1556.711	1557.367	1558.018	1558.693
$f_{\lambda_i}$ (nm) <sup>a</sup>	≤0.008	≤0.001	≤0.002	≤0.002	≤0.005	≤0.001	≤0.002	≤0.001
$f_{p_i}$ (dB) <sup>b</sup>	≤1.229	≤0.218	≤0.356	≤0.243	≤1.262	≤0.374	≤0.194	≤0.301
OSNR (dB)	>73	>73	>73	>72	>71	>63	>69	>63
SMSR (dB)	>56	>56	>56	>55	>54	>46	>53	>46

<sup>a</sup>  $f_{\lambda_i}$  ( $i = 1, 2, \dots, 8$ ): wavelength fluctuation of the  $\lambda_i$  lasing; <sup>b</sup>  $f_{p_i}$  ( $i = 1, 2, \dots, 8$ ): power fluctuation of the  $\lambda_i$  lasing.

Limited by the OSA resolution, the DSHMS is used to analyze the linewidth characteristics of lasers. In theory, the measurement resolution  $\Delta f$  of the DSHMS can be expressed as in [32]:

$$\Delta f = \frac{c}{n_{\text{eff}} \Delta L}, \tag{3}$$

where  $\Delta L$  is the length of the delay fiber.

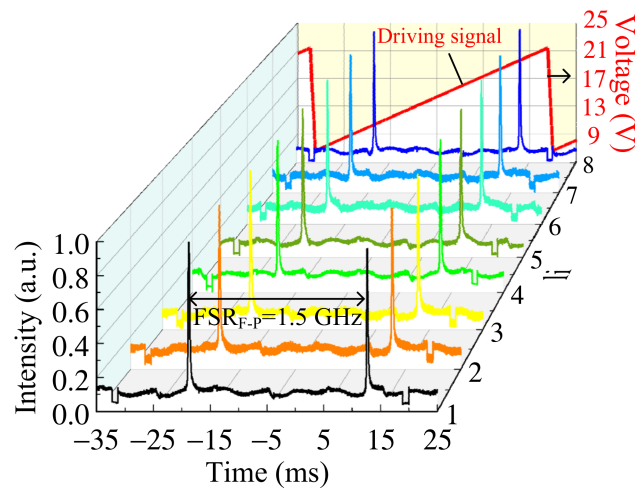


**Figure 4.** SLM operation performances of the eight single-wavelength operations measured by scanning the F-P interferometer.

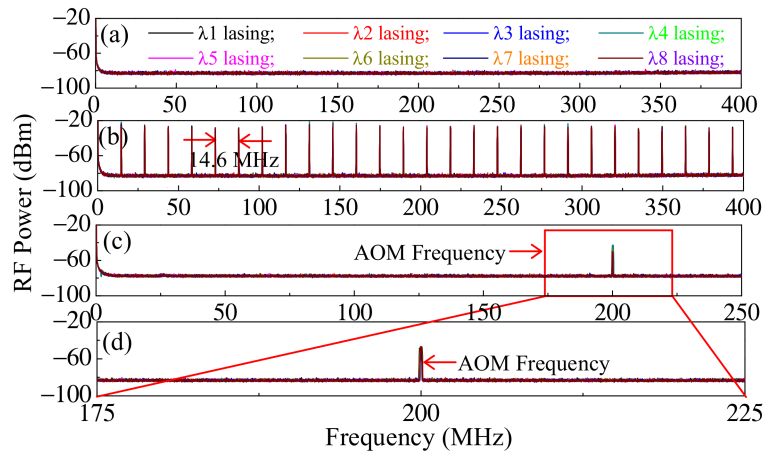


**Figure 5.** RF spectra of each single-wavelength lasing measured by the self-homodyne method using (a) MH mode in a range of 0–400 MHz for 10 min with a resolution bandwidth (RBW) of 51 kHz; and (b) MH mode in a range of 0–400 MHz for 10 min with an RBW of 51 kHz when the F-P and SCR filters are replaced by an SMF having the same efficient length. RF spectra measured by the delayed self-heterodyne method for almost 30 min using the MH mode are in (c) 0–250 MHz, with an RBW of 51 kHz; and (d) 175–225 MHz, with an RBW of 30 kHz.

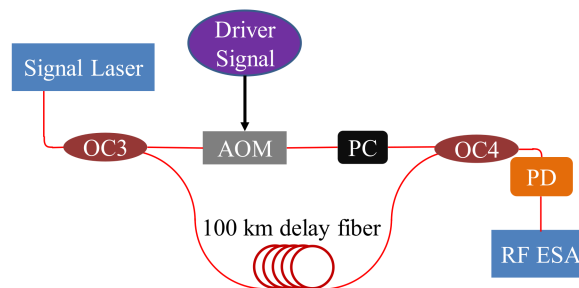


**Figure 6.** Schematic of the DSHMS.

Therefore, the calculated measurement resolution of the system is  $\sim 2.1$  kHz. The laser linewidths of the 8WS-EDFL at all lasing wavelengths were measured. Figure 7a,b, respectively, show the measurement data of the  $\lambda_2$  and  $\lambda_7$  lasings, as well as the Lorentz lineshape fitted curves of the corresponding data. As can be seen, the adjusted R-Square

(Adj. R-Square) values are, respectively, 0.958 and 0.967, and the 20-dB bandwidths are, respectively, 21.447 kHz and 21.558 kHz, which are both higher than the measurement resolution. The actual linewidth of a laser can be calculated as 1/20 times the 20-dB bandwidth of the fitted curve. Therefore, the linewidths of lasers  $\lambda_2$  and  $\lambda_7$  are 1072.35 Hz and 1077.90 Hz, respectively. The linewidths of the other lasers measured are shown in Table 2. It can be seen that all the laser linewidths of the single-wavelength operations are almost 1 kHz. It is important to mention that, when the incoherent mixing of lights from the two arms of the MZI occurred, the interference effect can lead to a spectrum broadening. However, it is not realistic to use a longer than 1000 km SMF delay line to achieve completely incoherent mixing due to the high fiber insertion loss. Consequently, considering the unavoidable broadening effects, the measurement linewidths should be larger than the intrinsic values of all lasers. The measured linewidths can be considered as the conservative values for determining the 8WS-EDFL's practical applications.

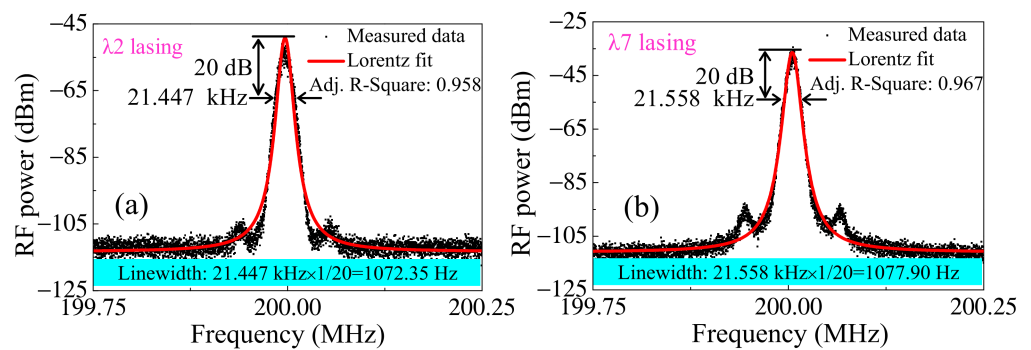


**Figure 7.** Linewidth measurements of the single-wavelength operations using DSHMS at (a)  $\lambda_2$  and (b)  $\lambda_7$  lasing, with the averaging mode for an RBW of 100 Hz.

**Table 2.** Linewidth measurement results for all the single-wavelength lasing outputs.

Lasing Wavelength	$\lambda_1$	$\lambda_2$	$\lambda_3$	$\lambda_4$	$\lambda_5$	$\lambda_6$	$\lambda_7$	$\lambda_8$
Adj. R-Square	0.969	0.969	0.967	0.960	0.968	0.961	0.967	0.963
Laser linewidth (Hz)	1131.25	1072.35	1094.70	1020.50	1025.70	959.55	1077.90	1011.70

To study the instantaneous power fluctuation of the laser output, the RIN spectra of the wavelength outputs at  $\lambda_2$  and  $\lambda_7$  are measured using a PD, an oscilloscope ((Tektronix, TDS2024C), used for measuring the direct voltage of the PD's output), and an ESA, as shown in Figure 8a,b. It can be seen that when the frequency is larger than 3 MHz, the RINs of the two lasers are less than or equal to  $-151.9$  dB/Hz and  $-152.1$  dB/Hz, respectively. In addition, the relaxation oscillation peaks of the two lasers are at 57.5 kHz and 52.0 kHz, as can be seen from the insets. The measurement results of other lasing wavelengths are shown in Table 3. The measured RIN values at all lasing wavelengths are  $\leq -150$  dB/Hz@  $\geq 3$  MHz, and the relaxation oscillation peaks are all between 51.8 kHz and 61.3 kHz. The differences for the different lasing wavelengths result from the different cavity losses for the different lasers and the small differences in the MRC's lengths under lasing at different channels of the CSI-HBFBG.

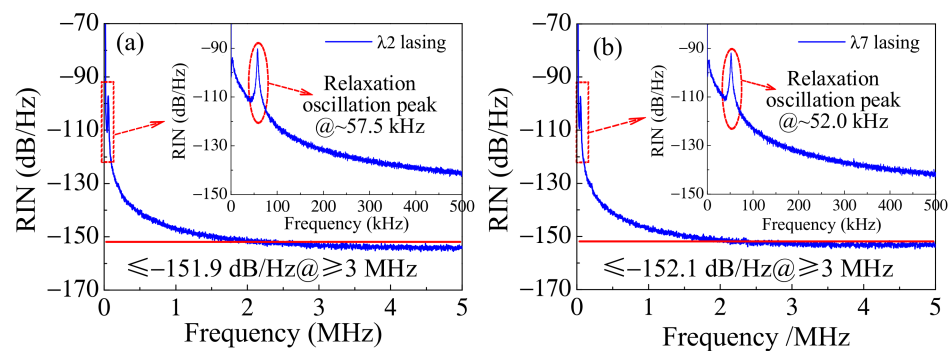


**Figure 8.** RIN spectra of the single-wavelength lasing operations at (a)  $\lambda_2$  and (b)  $\lambda_7$  in the range of 0–5 MHz, with an RBW of 10 kHz. The insets show the RIN spectra measured in the range of 0–500 kHz, with an RBW of 100 Hz, as well as the positions of the relaxation oscillation peaks of the lasers.

**Table 3.** RIN measurement results of the single-wavelength lasing outputs.

Lasing Wavelength	$\lambda_1$	$\lambda_2$	$\lambda_3$	$\lambda_4$	$\lambda_5$	$\lambda_6$	$\lambda_7$	$\lambda_8$
RIN@ $\geq 3$ MHz (dB/Hz)	−153.0	−151.9	−151.3	−150.8	−153.2	−153.4	−152.1	−152.7
Relaxation oscillation peak (kHz)	59.4	57.5	51.8	51.9	57.4	61.3	52.0	54.1

The output polarization characteristics of the eight single-wavelength operations were measured using a polarization analyzer (General Photonics Cor., PSY-201, Luna Innovations, Chino, CA, USA), as shown in Figure 9a–h. For each lasing wavelength, the PSY-201 was continuously measured for 5 min. For these measurements, the fiber pigtailed from the laser output port to the input port of the PSY-201 were fixed using soft adhesive tape. It can be seen that the degree of polarization (DOP) at each lasing wavelength is close to 100% (values slightly larger than 100% are mainly induced by the analysis error). The polarization states lasing at  $\lambda_1$ ,  $\lambda_3$ ,  $\lambda_5$ , and  $\lambda_7$  are almost orthogonal to those lasing at  $\lambda_2$ ,  $\lambda_4$ ,  $\lambda_6$ , and  $\lambda_8$ . In addition, we can see that, for the four lasers in the group of lasing at  $\lambda_1$ ,  $\lambda_3$ ,  $\lambda_5$ , and  $\lambda_7$ , or in the group of lasing at  $\lambda_2$ ,  $\lambda_4$ ,  $\lambda_6$ , and  $\lambda_8$ , the polarization states are almost parallel. This is consistent with the polarization states of the CSI-HBFBG's eight reflecting channels analyzed in Figure 2.

As described in Section 2, the channels 1, 3, 5, and 7 of the CSI-HBFBG reflect lights with the polarization state orthogonal to that of lights reflected by channels 2, 4, 6, and 8. Two lasers with the orthogonal polarization states can form the strongest PHB effect in the EDF and are with weakest gain competition. Therefore, by controlling the two TL-PCs to make any two lasers with orthogonal polarization states to be with lowest PDL at the CSI-HBFBG, a stable dual-wavelength operation can be obtained. We investigated all of the dual-wavelength operations with orthogonal polarization states at two lasing wavelengths. When the pump power was 200 mW, by adjusting two TL-PCs, 16 groups of dual-wavelength lasing combinations were achieved, which are lasing at  $\lambda_1$ & $\lambda_2$ ,  $\lambda_1$ & $\lambda_4$ ,  $\lambda_1$ & $\lambda_6$ ,  $\lambda_1$ & $\lambda_8$ ,  $\lambda_2$ & $\lambda_3$ ,  $\lambda_2$ & $\lambda_5$ ,  $\lambda_2$ & $\lambda_7$ ,  $\lambda_3$ & $\lambda_4$ ,  $\lambda_3$ & $\lambda_6$ ,  $\lambda_3$ & $\lambda_8$ ,  $\lambda_4$ & $\lambda_5$ ,  $\lambda_4$ & $\lambda_7$ ,  $\lambda_5$ & $\lambda_6$ ,  $\lambda_5$ & $\lambda_8$ ,  $\lambda_6$ & $\lambda_7$ , and  $\lambda_7$ & $\lambda_8$ , respectively, as shown in Figure 10. It can be seen that the OSNR of every dual-wavelength operation is higher than 65 dB. In addition, the lasing stability of every dual-wavelength operation measured was satisfying.

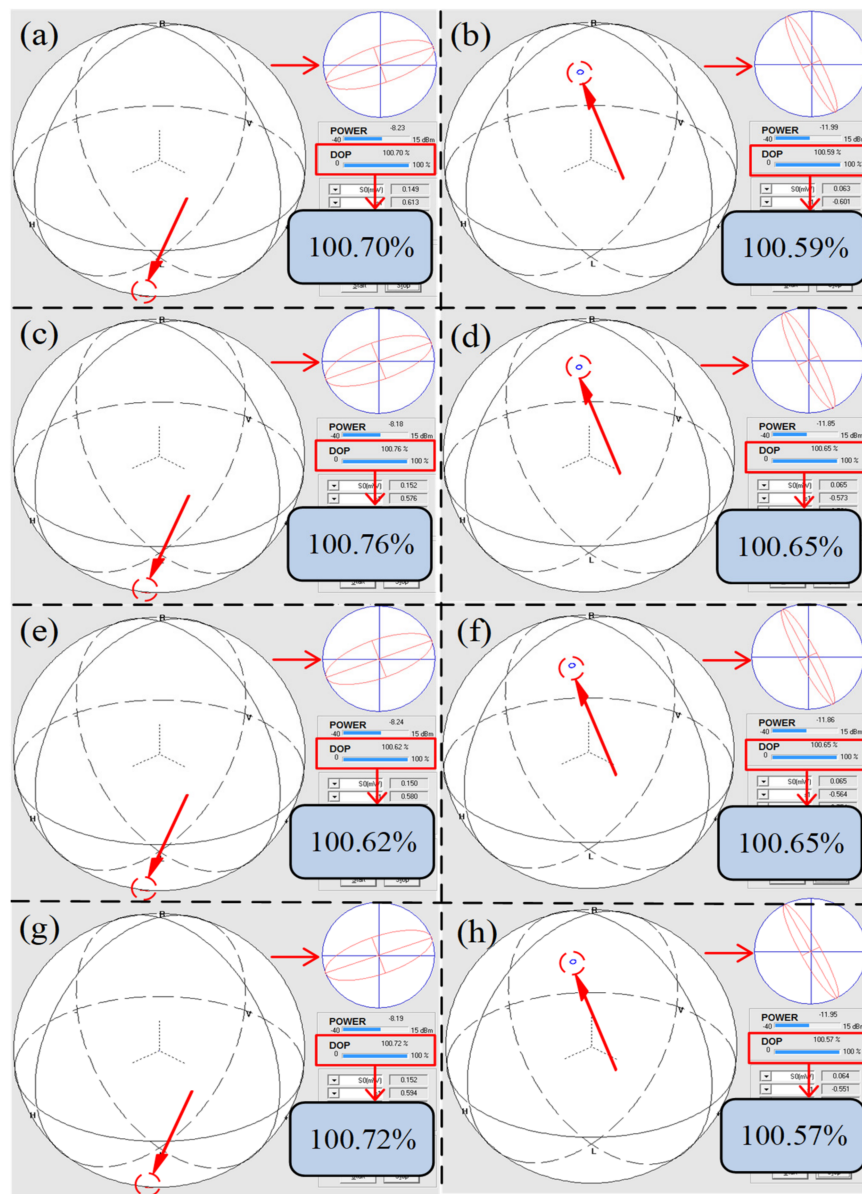


Figure 9. Measurements of the SOPs in single-wavelength lasing operations at (a)  $\lambda_1$ , (b)  $\lambda_2$ , (c)  $\lambda_3$ , (d)  $\lambda_4$ , (e)  $\lambda_5$ , (f)  $\lambda_6$ , (g)  $\lambda_7$ , and (h)  $\lambda_8$ .

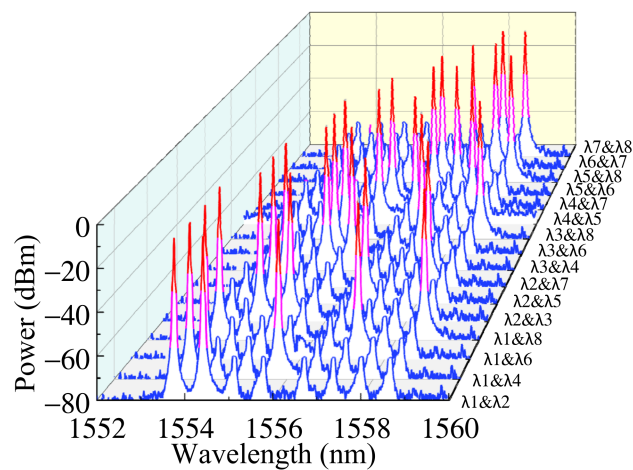


Figure 10. Spectra of the dual-wavelength switchable operation with orthogonal polarization states.

#### 4. Conclusions

In this paper, a high-performance SLM narrow-linewidth 8WS-EDFL is proposed and evaluated. Eight single-wavelength operations and sixteen dual-wavelength operations with orthogonal polarization states were obtained and can be switched to output. An CSI-HBFBG was used to determine the lasing wavelengths and the combination of an F-P filter and an SCR was used to select the SLM lasing. The output characteristics of the eight single-wavelength operations were studied in detail. When the pump power was 200 mW, the eight single-wavelength lasers were all in stable SLM oscillation, and they all had a linewidth of  $\sim 1$  kHz, an OSNR of  $>63$  dB, an  $\text{RIN} \leq -150$  dB/Hz@  $\geq 3$  MHz (close to the shot noise limit), and a high stability. The sixteen dual-wavelength operations with orthogonal polarization states all had an OSNR of  $>65$  dB and a stable spectrum. The proposed 8WS-EDFL has a simple structure and a high performance, and it will have better output characteristics after professional temperature compensation and vibration isolation packaging.

**Author Contributions:** Conceptualization, T.F.; methodology, T.F. and F.Y.; software, D.L.; validation, D.L. and W.S.; resources, T.F., F.Y. and X.S.Y.; data curation, T.F. and D.L.; writing—original draft preparation, D.L. and W.S.; writing—review and editing, T.F., S.W. and Q.L.; supervision, T.F. and X.S.Y.; project administration, T.F. All authors have read and agreed to the published version of the manuscript.

**Funding:** This work was supported by the National Natural Science Foundation of China (Grant Nos. 61975049 and 61827818), the Natural Science Foundation for Outstanding Young Scholars of Hebei Province, China (Grant No. F2020201001), the Program of “333 talent project” of Hebei Province, China (Grant No. A202101010), and the Creative Ability Improvement Program of Hebei Province, China (Grant No. 20542201D).

**Institutional Review Board Statement:** Not applicable.

**Informed Consent Statement:** Not applicable.

**Data Availability Statement:** The data presented in this study may be available from the corresponding author upon reasonable request.

**Conflicts of Interest:** The authors declare no conflict of interest.

#### References

1. Kumar, C.; Kumar, G. S + C double-band flattened gain hybrid optical amplifier [RAMAN + thulium-doped photonic crystal fiber amplifier (TD-PCFA)] for super-dense wavelength division multiplexing system. *J. Opt.* **2020**, *49*, 178–180. [[CrossRef](#)]
2. Cai, X.; Luo, J.; Fu, H.; Bu, Y.; Chen, N. Temperature measurement using a multi-wavelength fiber ring laser based on a hybrid gain medium and Sagnac interferometer. *Opt. Express* **2020**, *28*, 39933–39943. [[CrossRef](#)] [[PubMed](#)]
3. Al-Taiy, H.; Wenzel, N.; Preussler, S.; Klinger, J.; Schneider, T. Ultra-narrow linewidth, stable and tunable laser source for optical communication systems and spectroscopy. *Opt. Lett.* **2014**, *39*, 5826–5829. [[CrossRef](#)] [[PubMed](#)]
4. Tai, Z.-Y.; Yan, L.-L.; Zhang, Y.-Y.; Zhang, X.-F.; Guo, W.-G.; Zhang, S.-G.; Jiang, H.-F. Transportable 1555-nm Ultra-Stable Laser with Sub-0.185-Hz Linewidth. *Chin. Phys. Lett.* **2017**, *34*, 090602. [[CrossRef](#)]
5. Kessler, T.; Hagemann, C.; Grebing, C.; Legero, T.; Sterr, U.; Riehle, F.; Martin, M.J.; Chen, L.; Ye, J. A sub-40-mHz-linewidth laser based on a silicon single-crystal optical cavity. *Nat. Photonics* **2012**, *6*, 687–692. [[CrossRef](#)]
6. Yang, A.; Wang, T.; Zheng, J.; Zeng, X.; Pang, F.; Wang, T. A single-longitudinal-mode narrow-linewidth dual-wavelength fiber laser using a microfiber knot resonator. *Laser Phys. Lett.* **2019**, *16*, 025104. [[CrossRef](#)]
7. Shen, Z.; Wang, L.; Wang, X.; Cao, Y.; Feng, X.; Guan, B.-o. Tunable dual-wavelength single-longitudinal-mode fiber laser based on spectral narrowing effect in a nonlinear semiconductor optical amplifier. *Opt. Laser Technol.* **2017**, *94*, 72–76. [[CrossRef](#)]
8. Cheng, D.; Yan, F.; Feng, T.; Zhang, L.; Han, W.; Qin, Q.; Li, T.; Bai, Z.; Yang, D.; Guo, Y.; et al. Six-Wavelength-Switchable SLM Thulium-Doped Fiber Laser Enabled by Sampled FBGs and  $3 \times 3$  Coupler Based Dual-Ring Compound Cavity Filter. *IEEE Photonics J.* **2022**, *14*, 1515908. [[CrossRef](#)]
9. Zhang, L.; Yan, F.; Feng, T.; Han, W.; Guan, B.; Qin, Q.; Guo, Y.; Wang, W.; Bai, Z.; Zhou, H.; et al. Six-wavelength-switchable narrow-linewidth thulium-doped fiber laser with polarization-maintaining sampled fiber Bragg grating. *Opt. Laser Technol.* **2021**, *136*, 106788. [[CrossRef](#)]
10. Feng, T.; Wei, D.; Bi, W.; Sun, W.; Wu, S.; Jiang, M.; Yan, F.; Suo, Y.; Yao, X.S. Wavelength-switchable ultra-narrow linewidth fiber laser enabled by a figure-8 compound-ring-cavity filter and a polarization-managed four-channel filter. *Opt. Express* **2021**, *29*, 31179–31200. [[CrossRef](#)]

11. Feng, T.; Jiang, M.; Wei, D.; Zhang, L.; Yan, F.; Wu, S.; Yao, X.S. Four-wavelength-switchable SLM fiber laser with sub-kHz linewidth using superimposed high-birefringence FBG and dual-coupler ring based compound-cavity filter. *Opt. Express* **2019**, *27*, 36662–36679. [[CrossRef](#)]
12. Hsu, Y.; Chang, Y.C.; Yeh, C.H.; Chow, C.W.; Chen, J.H. Based on Silicon-Micro-Ring-Resonator and Triple-Ring Cavity for Stable and Tunable Erbium Fiber Laser. In Proceedings of the 2018 Progress in Electromagnetics Research Symposium (PIERS-Toyama), Toyama, Japan, 1–4 August 2018; pp. 1399–1404. [[CrossRef](#)]
13. Zhou, X.; Li, Z.; Zhou, Y. Tunable and switchable multi-wavelength fiber laser based on polarization hole burning effect and Sagnac loop mirrors. *Opt. Quantum Electron.* **2020**, *52*, 451. [[CrossRef](#)]
14. Zhang, L.; Tian, Z.; Chen, N.-K.; Han, H.; Liu, C.-N.; Grattan, K.T.V.; Rahman, B.M.A.; Zhou, H.; Liaw, S.-K.; Bai, C. Room-Temperature Power-Stabilized Narrow-Linewidth Tunable Erbium-Doped Fiber Ring Laser Based on Cascaded Mach-Zehnder Interferometers With Different Free Spectral Range for Strain Sensing. *J. Light. Technol.* **2020**, *38*, 1966–1974. [[CrossRef](#)]
15. Martin-Vela, J.A.; Sierra-Hernandez, J.M.; Gallegos-Arellano, E.; Estudillo-Ayala, J.M.; Bianchetti, M.; Jauregui-Vazquez, D.; Reyes-Ayona, J.R.; Silva-Alvarado, E.C.; Rojas-Laguna, R. Switchable and tunable multi-wavelength fiber laser based on a core-offset aluminum coated Mach-Zehnder interferometer. *Opt. Laser Technol.* **2020**, *125*, 106039. [[CrossRef](#)]
16. Gao, S.; Jing, Z.; Chen, H. A stable three-wavelength ring-cavity laser based on SOA with two FBGs and a DFB laser injection. *Opt. Laser Technol.* **2020**, *130*, 106362. [[CrossRef](#)]
17. Yang, X.; Lindberg, R.; Margulis, W.; Frojdh, K.; Laurell, F. Continuously tunable, narrow-linewidth laser based on a semiconductor optical amplifier and a linearly chirped fiber Bragg grating. *Opt. Express* **2019**, *27*, 14213–14220. [[CrossRef](#)]
18. Zhao, Q.; Pei, L.; Wang, J.; Xie, Y.; Ruan, Z.; Zheng, J.; Li, J.; Ning, T. Interval-Adjustable Multi-Wavelength Erbium-Doped Fiber Laser With the assistance of NOLM or NALM. *IEEE Access* **2021**, *9*, 16316–16322. [[CrossRef](#)]
19. Jasim, A.A.; Dernaika, M.; Harun, S.W.; Ahmad, H. A Switchable Figure Eight Erbium-Doped Fiber Laser Based on Inter-Modal Beating By Means of Non-Adiabatic Microfiber. *J. Light. Technol.* **2015**, *33*, 528–534. [[CrossRef](#)]
20. Zhao, Q.; Pei, L.; Tang, M.; Xie, Y.; Ruan, Z.; Zheng, J.; Ning, T. Switchable multi-wavelength erbium-doped fiber laser based on core-offset structure and four-wave-mixing effect. *Opt. Fiber Technol.* **2020**, *54*, 102111. [[CrossRef](#)]
21. Zhang, C.; Sun, J.; Jian, S. A new mechanism to suppress the homogeneous gain broadening for stable multi-wavelength erbium-doped fiber laser. *Opt. Commun.* **2013**, *288*, 97–100. [[CrossRef](#)]
22. Tao, Y.; Zhang, S.; Jiang, M.; Li, C.; Zhou, P.; Jiang, Z. High power and high efficiency single-frequency 1030 nm DFB fiber laser. *Opt. Laser Technol.* **2022**, *145*, 107519. [[CrossRef](#)]
23. Tan, T.; Yang, C.; Wang, W.; Wang, Y.; Zhao, Q.; Guan, X.; Peng, M.; Gan, J.; Yang, Z.; Xu, S. Ultralow-intensity-noise single-frequency fiber-based laser at 780 nm. *Appl. Phys. Express* **2020**, *13*, 022002. [[CrossRef](#)]
24. Huang, L.; Yang, C.; Tan, T.; Lin, W.; Zhang, Z.; Zhou, K.; Zhao, Q.; Teng, X.; Xu, S.; Yang, Z. Sub-kHz-Linewidth Wavelength-Tunable Single-Frequency Ring-Cavity Fiber Laser for C- and L-Band Operation. *J. Light. Technol.* **2021**, *39*, 4794–4799. [[CrossRef](#)]
25. Feng, T.; Wang, M.; Wang, X.; Yan, F.; Suo, Y.; Yao, X.S. Switchable 0.612-nm-Spaced Dual-Wavelength Fiber Laser With Sub-kHz Linewidth, Ultra-High OSNR, Ultra-Low RIN, and Orthogonal Polarization Outputs. *J. Light. Technol.* **2019**, *37*, 3173–3182. [[CrossRef](#)]
26. Xie, Y.-R.; Luo, C.-M.; Yeh, C.-H. Use of C-band erbium gain-medium and compound-fiber-ring design for single-longitudinal-mode fiber laser with 84-nm achievable tunability. *Opt. Fiber Technol.* **2019**, *52*, 101974. [[CrossRef](#)]
27. Wei, F.; Yang, F.; Zhang, X.; Xu, D.; Ding, M.; Zhang, L.; Chen, D.; Cai, H.; Fang, Z.; Xijia, G. Subkilohertz linewidth reduction of a DFB diode laser using self-injection locking with a fiber Bragg grating Fabry-Perot cavity. *Opt. Express* **2016**, *24*, 17406–17415. [[CrossRef](#)]
28. Yin, B.; Feng, S.; Liu, Z.; Bai, Y.; Jian, S. Tunable and switchable dual-wavelength single polarization narrow linewidth SLM erbium-doped fiber laser based on a PM-CMFBG filter. *Opt. Express* **2014**, *22*, 22528–22533. [[CrossRef](#)]
29. Wang, Z.; Wang, Q.; Zhang, W.; Wei, H.; Li, Y.; Ren, W. Ultrasensitive photoacoustic detection in a high-finesse cavity with Pound-Drever-Hall locking. *Opt. Lett.* **2019**, *44*, 1924–1927. [[CrossRef](#)]
30. Zhang, J.; Yue, C.Y.; Schinn, G.W.; Clements, W.; Lit, J. Stable single-mode compound-ring erbium-doped fiber laser. *J. Light. Technol.* **2002**, *14*, 104–109. [[CrossRef](#)]
31. Zhang, L.; Zhang, J.; Sheng, Q.; Shi, C.; Shi, W.; Yao, J. Watt-level 1.7- $\mu\text{m}$  single-frequency thulium-doped fiber oscillator. *Opt. Express* **2021**, *29*, 27048–27056. [[CrossRef](#)]
32. Horak, P.; Loh, W.H. On the delayed self-heterodyne interferometric technique for determining the linewidth of fiber lasers. *Opt. Express* **2006**, *14*, 3923–3928. [[CrossRef](#)]